A simple acrylic acid functionalized zinc porphyrin for cost-effective dye-sensitized solar cells

Hongshan He[1*], Ashim Gurung[1], Liping Si[1] and Andrew G. Sykes[2]

[1]Center for Advanced Photovoltaics, South Dakota State University, Brookings, SD 57007, USA; [2]Department of Chemistry, University of South Dakota, Vermilion, SD 56069, USA.

Experimental section

All solvents were treated by standard methods prior to use. All chemicals were analytical grade and used as received. The FTO (fluorine-tine-oxide) glass with sheet resistance 8 Ω/cm^2 from Hartfort Glass (USA) was used for cell fabrication. 5,15-dimesitylporphyrin zinc (DMPZn-Br) and 5-(4-carboxylpheny)-10, 15,20-triphenylporphyrin zinc (TPPZn-COOH) was prepared as described previously.[1]Absorption spectra were obtained on an HP Agilent 8543 UV-visible spectrophotometer in CH_3CN at room temperature. The steady-state fluorescence spectra were obtained on a fluorimeter (FS920, Edinburg Instrument, Inc, UK) with a Xenon arc lamp as light source. The decay curves of fluorescence were measured on a fluorimeter using time-correlated single-photon-counting technique (LifeSpec II, Edinburg Instrument, Inc.). The diode laser (EPL 375, Edinburg Instrument, Inc, UK) with wavelength at 375 nm was used as light source. The pulse repetition frequency was 20 MHz. The lifetimes were obtained by exponential fitting of deconvoluted decay curves.

Synthesis of DMPZn-C2-COOH

To DMPZn-Br (0.08 mmol), $Pd(OAc)_2$ (0.016 mmol), Cs_2CO_3 (0.8 mmol) and Ph_3P (0.24 mmol) in a pressure tube was added extra dry toluene (10 ml) under nitrogen atmosphere. Then methyl acrylate (0.8 mmol) was added and the tube was sealed by a cap. The tube was put in an oil bath at 80ºC for 24h. Then the tube was cooled to room temperature and solution was transferred to a round-bottom flask and solvent was removed on a rotor evaporator. The solid was re-dissolved in chloroform and the product was purified on silica gel using chloroform as elute. The major band (second band) was collected and the solvent was removed. The solid (0.05 mmol) was dissolved in ethanol (10 ml) in a pressure tube. Then KOH aqueous solution (1.0 ml, 1.0 mol/L) was added. The tube was sealed and was put in an oil bath at 80ºC for 12h. Then the solvent was removed and the solid was washed with ~1.0 M HCl aqueous solution and with DI water several times. The solid was collected and dried in vacuum. ^{1}H NMR (CD_3OD, ppm): 10.25 (1H, d, alkene), 9.42 (2H, d, ß pyrrole), 8.93 (2H, d, ß pyrrole), 8.81 (2H, d, ß pyrrole), 8.78 (2H, d, ß pyrrole), 7.52 (4H, s, Phen), 6.84 (1H, d, alkene H), 2.61 (6H, s, *p*-CH_3), 1.72 (12H, s, *o*-CH_3). ES MS: m/z, 677.09 (M-1) $C_{41}H_{34}N_4O_2Zn$ (678.20). Elemental analysis: found C 70.54, H 5.10, N 8.02; $C_{40}H_{34}N_4O_2Zn$ CH_3OH, requires C 70.83, H 5.38, N 7.87%.

X-ray crystallographic analysis

Single crystals of DMPZn-Br were obtained by slow evaporation of solvent from the respective complexes in 1:1 (v:v) mixtures of methanol and dichloromethane at room temperature. A crystal was mounted on glass fibers for data collection. Diffraction measurements were made on a CCD-based commercial X-ray diffractometer using Mo Kα radiation (λ= 0.71073 Å). The frames were collected at 125 K with a scan width 0.3° in ω and integrated with Bruker SAINT software package using narrow-frame integration algorithm. The unit cell was determined and refined by least squares upon the refinement of XYZ-centeroids of reflections above 20σ(I). The data were corrected for absorption using SADABS program. The structures were refined on F^2 using the Bruker SHELXTL (version 5.1) software package.[2,3] Crystal data for DMPZn-Br: $C_{38}H_{31}BrN_4Zn$, MW = 688.95, triclinic, space group = P-1, a = 7.1655(6), b =12.8935(10), c = 16.6030(10) Å, α = 84.0560(10), β = 79.6630 (10), γ = 82.57520(10)°, V = 1202.7(2) Å^3, Z = 2, ρ_{calcd}. = 1.534 Mgm^{-3}, μ(Mo-Kα) = 2.1998 mm^{-1}, F(000) = 704, T = 100(2) K. 14215 reflections were measured, of which 5295 were unique (Rint = 0.0280). Final R_1 = 0.0306 and wR1 = 0.0.0820 values were obtained for 5259 observed reflections with I>2σ(I), 411 parameters, and GOF = 1.039. The overall quality of the structure was not good; however, it is clear that OQ unit was linked to the porphyrin successfully. The porphyrin is disordered rotationally around the mesityl group's 2-fold axis producing two bromine occupancies in a 93:7 ratio. The minor bromine occupancy was kept isotropic and the minor occupancy of the corresponding hydrogen on the opposite side of the porphyrin ring was not found from the difference map and was unstable if put in a calculated position.

Fabrication of DSCs

The nanocrystalline TiO_2 paste from the Dyesol was coated on a commercial fluorine-tin-oxide (FTO) using doctor-blade method. After air-drying for about 30 minutes, the sample was put into an oven for sintering (500°C for 30 min) in ambient oxygen. The samples were then coated a scattering layer with larger size (diameter ~ 400 nm) and sintered again at 500°C for 30 minutes. The sample was then cooled to the room temperature and was immersed in a $TiCl_4$ aqueous solution (20 mM) for one hour. The film was air-dried and sintered again at 500°C for 30 minutes. The film was then put into the dye solution (~ 0.3 mM in methanol) at room temperature and kept for four hour. The film was then taken out, flushed with methanol, and vacuum dried for one hour. The thickness of the film was ~ 6.6 µm from cross-view images of scanning electron microscope (SEM). The counter-electrode was prepared by sputtering a 16 nm-thick film of the Pt on the FTO glass. A mask made from the Parafilm was used as a spacer for two electrodes and sealing material. The electrolyte solution was injected from two pre-cut channels in the mask. The outside of the final cell was sealed by hot glue. The electrolyte is an acetonitrile solution having 0.6 M 1-propyl-2,3-dimethylimidazolium iodide, 0.05 M I_2, 0.1 M LiI, 0.1 M guanidine thiocyanate and 0.5 M *tert*-butylpyridine.

Solar cell characterization

The applied potential and cell current were measured using an Agilent 4155C semiconductor parameter analyzer using a 450W Xenon light source. The light intensity at the surface of cell was calibrated to 100 mW/cm^2, equivalent to one sun at air mass 1.5G condition. Efficiency (η) and the fill factor (ff) were calculated by η (%) = $P_{max} \times 100/(P_{in} \times A)$ and FF = $P_{max}/(I_{SC} \times V_{OC})$, where P_{max} is the maximum output power of cells (mW), Pin is the power density of the light source (mW/cm^2), Isc is the short-circuit current (mA), V_{oc} is the open-circuit voltage (V), A is the active area (0.16 cm^2) of the cell. Incident photon to charge carrier efficiency (IPCE) experiments were performed on an Agilent semiconductor parameter analyzer with an Xe arc lamp and an Newport monochromator. Monochromatic light was incident on the sample through focusing lenses. The National Renewable Energy Laboratory (NREL) calibrated photodetector was used as a reference. The samples were scanned from 350 - 850 nm and the voltage was recorded. The IPCE was calculated using the equation IPCE = (Sample Voltage × Reference voltage)/Reference IPCE. The reference IPCE was supplied by the NREL calibrated DSSC under AM1.5 photon flux. Electron impedance spectroscopy (EIS) measurements were performed on an HP 4192A LF impedance analyzer (5 Hz-13 MHz) set up in two electrode configuration. 10

mV of AC perturbation was applied ranging between 5 - 10^5 Hz. The measurements were performed in dark under forward bias condition from 0 to 1 V. A simplified Randles type model was used to fit the data to extract the series resistance (R_S), which accounts for transport resistance of TCO, the combined charge transfer resistance for electron recombination at TCO/electrolyte and TiO_2/electrolyte interface (R_{ct}), and the constant phase element representing capacitance at TCO/electrolyte/TiO_2 interface (CPE).

Dye-loading experiments

The dye loading densities were obtained by monitoring changes of the absorbance of TMPZn and BET in EtOH in a 1.0 cm cuvette in the presence of freestanding TiO_2 film. The film was placed at the bottom of the cuvette. The cuvette was sealed and absorption spectrum was recorded every 10 minutes. The mole number of dye molecules adsorbed on the TiO_2 surface (Q_t, mol/cm^2) at the time t (min) was calculated using following equation:[3-5]

$$Q_t = \frac{(C_0 - C_t) \times V}{m \times A}$$

where C_0 is the initial concentration of dye solution, C_t is the concentration of the dye solution at the time t, m is the weight of the TiO_2 film, V is the total volume of the solution, and A is the surface area of the TiO_2 nanoparticles (70 cm^2/g). The amount of adsorbed dye on the TiO_2 film at equilibrium (Q_e) was obtained by fitting the data using the pseudo-first order model:

$$Q_t = Q_e - Q_e e^{-kt}$$

where k (min^{-1}) is the first order adsorption constant.

Theoretical calculations

The theoretical calculations were performed at density functional theory level. The single-crystal structures were used as framework for the construction of initial input structures of calculations. Geometry optimization and electronic structure calculations were performed using B3LYP functional and 6-31d(d) basis set in acetonitrile solution by means of the conductor-like polarizable continuum model (CPCM) solvation model, as implemented in the Gaussian 09[6] program package. The acetonitrile was used to mimic the solvents in electrolyte. Molecular orbitals were visualized by GaussView 3.0 software. The method has been used widely for geometry optimization and electronic calculations of porphyrins derivatives for its accuracy, which was further validated by very similar bond angles and bond lengths in optimized structures of DMPZn-Br to its single-crystal structures.

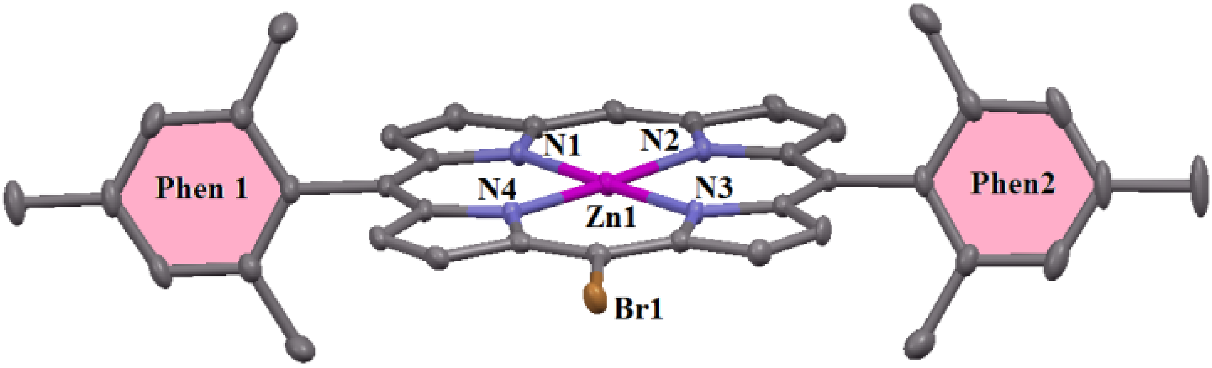

Fig. S1 ORTEP diagram of DMPZn-Br with 50% thermal ellpsoid probability. The torsion between Phen1 and Phen2 to porphyrin are 78.97º and 72.53º, respectively. Selected bond lengths (Å): Zn1-N1 = 2.024(2), Zn1-N2 = 2.031(2), Zn1-N3 = 2.034(2), Zn1-N4 = 2.033(2).

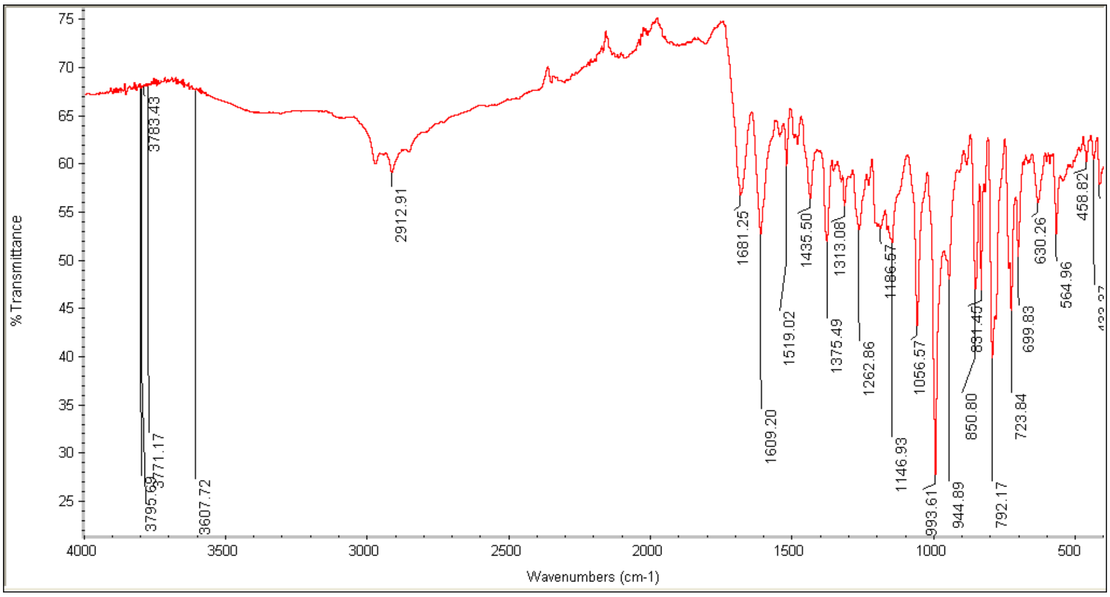

Figure S2. FT-IR spectra of DMPZn-C2-COOH

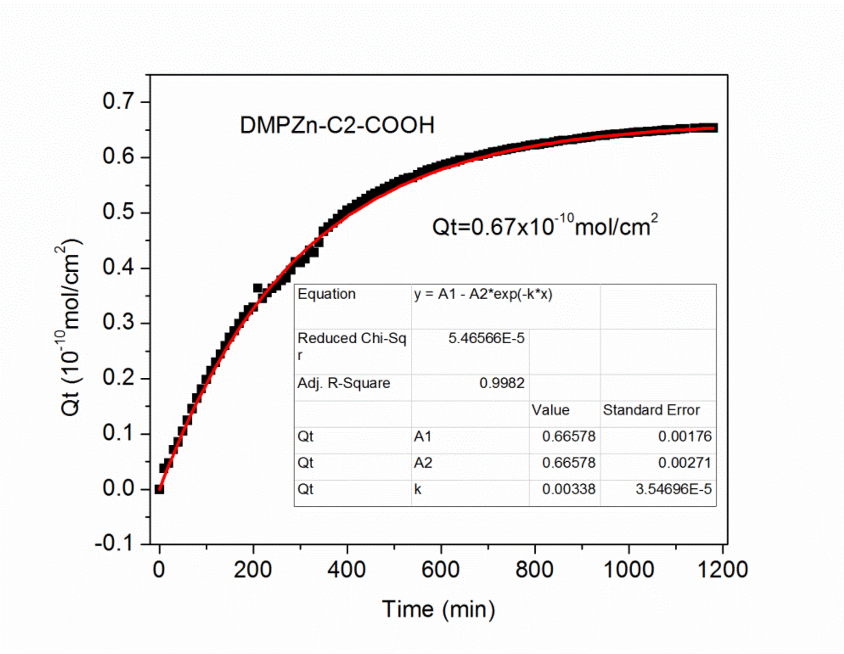

Figure S3. Typical dye-loading profiles of DMPZn-C2-COOH/BET on TiO_2 film at room temperature. The total dye loading density Qt was 0.67 $\times 10^{-10}$ mol/cm^2. The loading density after 4 hours immersing was 0.35 $\times 10^{-10}$ mol/cm^2

Table S1. Photovoltaic parameters of DMPZn-C2-COOH/BET sensitized solar cells using of cocktail dye loading.

Time (hour)	Ratio[a]	J_{SC} (mA/cm^2)	V_{OC} (mV)	FF	η (%)
4	0:1	0.52	470	0.670	0.16
4	1:0	6.67	650	0.700	3.02
4	1:3	3.94	590	0.729	1.68
4	1:1	4.95	602	0.732	2.18
4	1:0.5	7.01	612	0.721	3.10
4	1:0.1	7.37	623	0.713	3.27
8	1:0	5.99	641	0.714	2.74
8	1:0.5	5.77	610	0.705	2.48
8	1:0.1	6.48	640	0.698	2.89
12	1:0	5.83	632	0.700	2.58
12	1:0.5	5.40	604	0.737	2.40
12	1:0.1	6.62	632	0.710	2.96

[a] The molar ratio between DMPZn-C2-COOH and BET. The concentration of porphyrin was 0.3 mM.

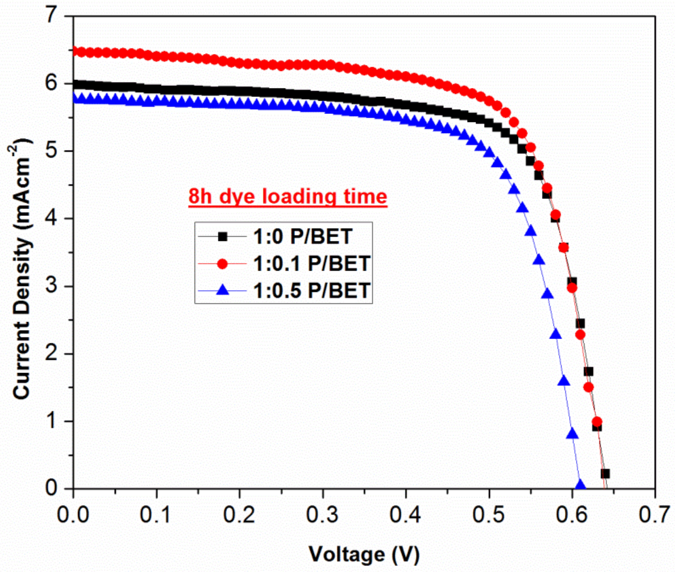

Figure S4. The *J-V* curves of DMPZn-C2-COOH with different molar ratio of BET under 8 h dye loading time using a cocktail method. P stands for DMPZn-C2-COOH.

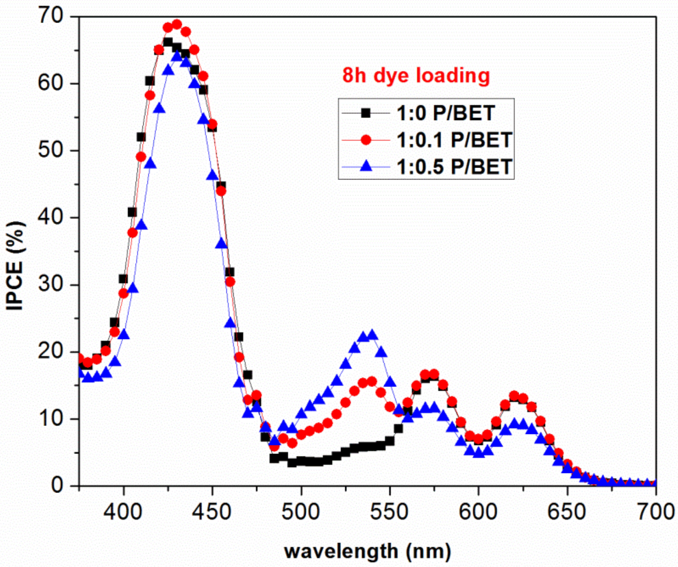

Figure S5. The IPCE curves of DMPZn-C2-COOH with different molar ratio of BET under 8 h dye loading time using a cocktail method. P stands for DMPZn-C2-COOH.

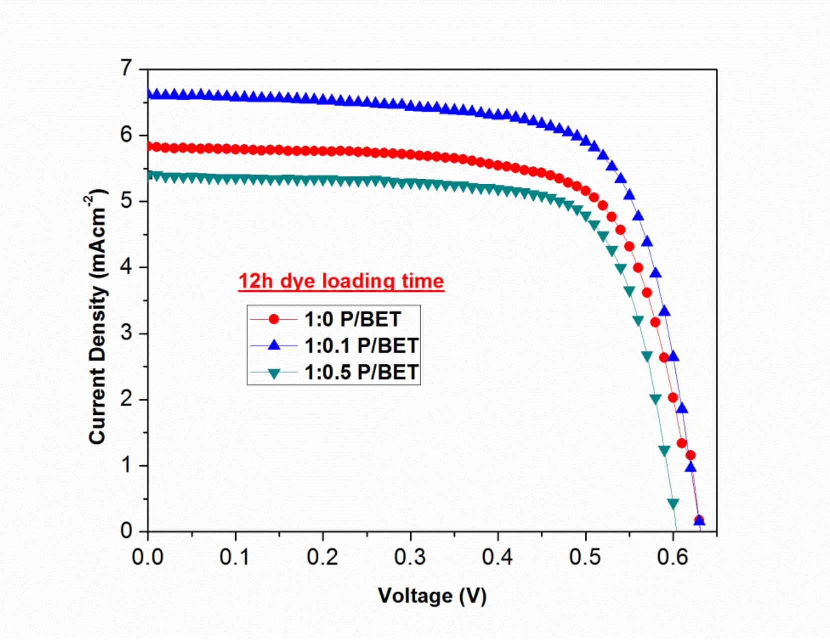

Figure S6. The *J-V* curves of DMPZn-C2-COOH with different molar ratio of BET under 12 h dye loading time using a cocktail method. P stands for DMPZn-C2-COOH.

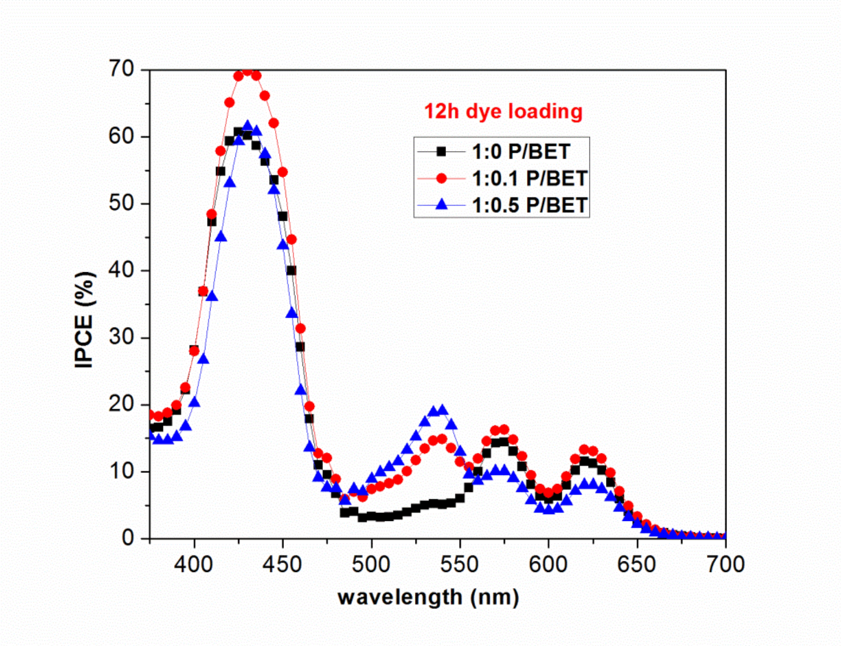

Figure S7. The IPCE curves of DMPZn-C2-COOH with different molar ratio of BET under 12 h dye loading time using a cocktail method. P stands for DMPZn-C2-COOH.

Table S2. Photovoltaic parameters of DMPZn-C2-COOH/BET sensitized solar cells using of sequential dye loading.

DMPZn-C2-COOH (minutes)	BET (minutes)	J_{SC} (mA/ cm^2)	V_{OC} (mV)	FF	η (%)
-	240	0.52	470	0.670	0.16
240	-	6.67	650	0.700	3.02
240	240	2.63	530	0.703	0.98
240	180	3.03	530	0.710	1.14
240	120	3.05	570	0.723	1.25
240	60	3.60	570	0.718	1.48
240	10	5.32	600	0.712	2.27
240	5	5.34	600	0.717	2.30
240	2	5.63	620	0.723	2.52

The concentration of porphyrin and BET was 0.3 mM.

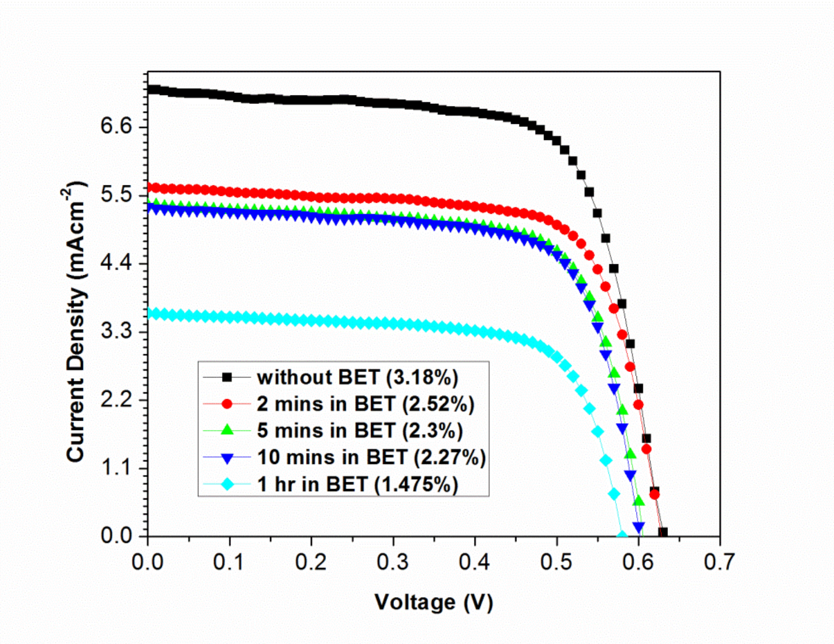

Figure S8. The *J-V* curves of DMPZn-C2-COOH with different molar ratio of BET using a sequential dyeing method.

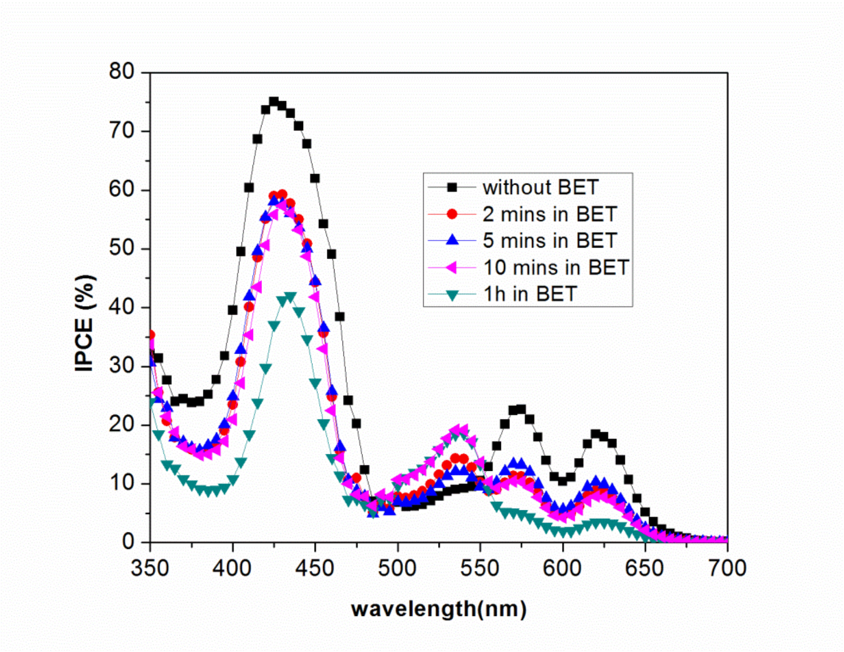

Figure S9. The IPCE curves of DMPZn-C2-COOH with different molar ratio of BET using a sequential dyeing method.

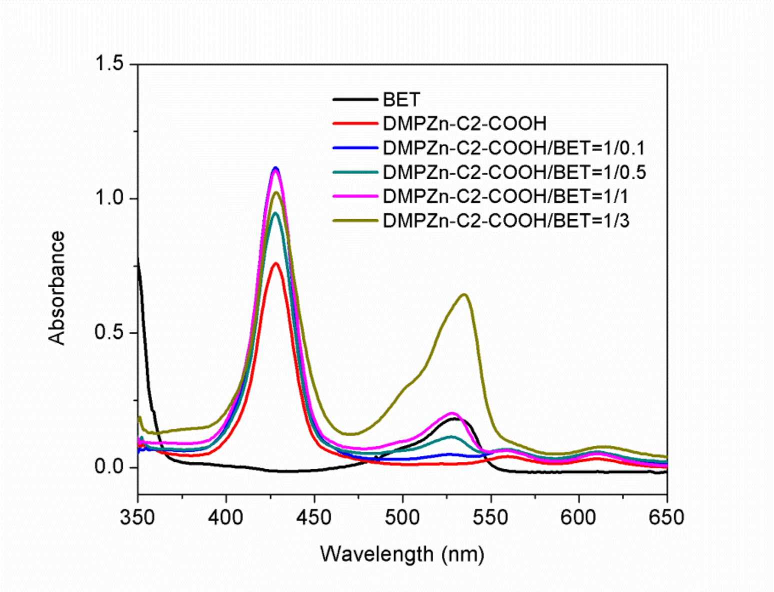

Figure S10. Absorption spectra of DMPZn-C2-COOH/BET with different molar ratio on TiO_2 films. The spectra were obtained by dipping TiO2 films into dye solutions for 30 seconds and flushing with ethanol. The film was then dipped into a quartz cell with pure CH_3CN and spectra were then recorded

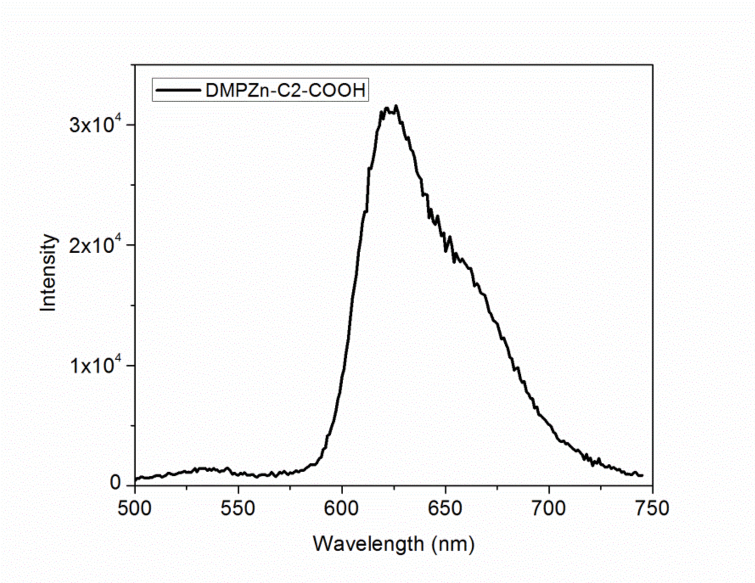

.

Figure S11. Fluorescence spectrum of DMPZn-C2-COOH in CH_2Cl_2 solution at room temperature. The concentration of the sample was 1.08×10^{-5} mol/L. The excitation wavelength was 375 nm.

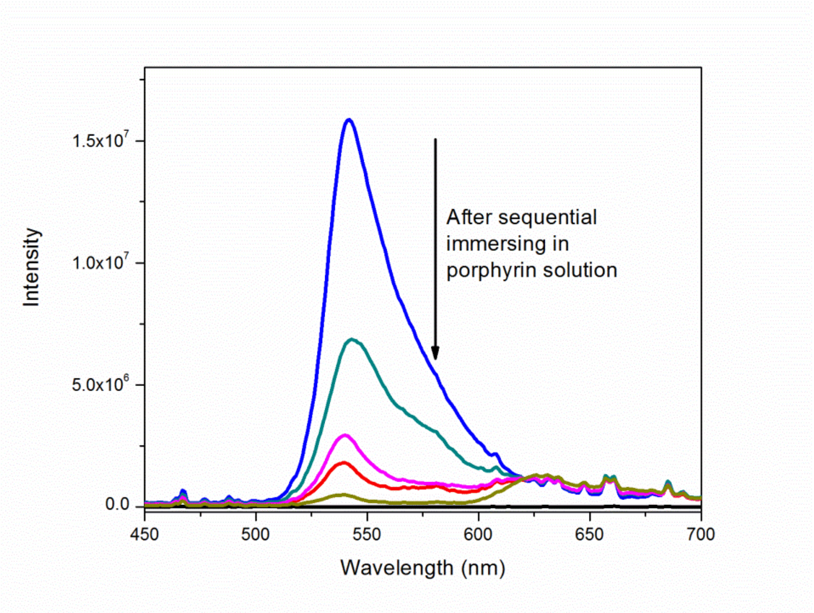

Figure S12. Changes of fluorescence spectra of BET coated Al_2O_3 film after co-adsorption of DMPZn-C2-COOH.

References

1.He, H.; Zhong, L.; Lin, Y.; Huang, L., New methods for the synthesis of 5-(2-hydroxyphenyl)-10,15,20-triphenylporphyrin and its derivatives. *Chem. Reagent* **2001,** 23(3), , (3), 169-170, 172.

2.Sheldrick, G. M., *Acta Cryst.* **2008,** A64, 112.

3.Pang, X.-Y.; Gong, F., Study on the Adsorption Kinetics of Acid Red 3B on Expanded Graphite. *E-J. Chem.* **2008,** 5, (4), 802-809.

4.Rudzinski, W.; Plazinski, W., Kinetics of Dyes Adsorption at the Solid-Solution Interfaces: A Theoretical Description Based on the Two-Step Kinetic Model. *Environ. Sci. Technol.* **2008,** 42, 2470-2475.

5.Azizian, S.; Bashiri, H., Description of Desorption Kinetics at the Solid/Solution Interface Based on the Statistical Rate Theory. *Langmuir* **2008,** 24, 13013-13018.

6.Frisch, M. J. T., G. W.; Schlegel, H. B.; Scuseria, G. E.; Robb, M. A.; Cheeseman, J. R.; Scalmani, G.; Barone, V.; Mennucci, B.; Petersson, G. A.; Nakatsuji, H.; Caricato, M.; Li, X.; Hratchian, H. P.; Izmaylov, A. F.; Bloino, J.; Zheng, G.; Sonnenberg, J. L.; Hada, M.; Ehara, M.; Toyota, K.; Fukuda, R.; Hasegawa, J.; Ishida, M.; Nakajima, T.; Honda, Y.; Kitao, O.; Nakai, H.; Vreven, T.; Montgomery, Jr., J. A.; Peralta, J. E.; Ogliaro, F.; Bearpark, M.; Heyd, J. J.; Brothers, E.; Kudin, K. N.; Staroverov, V. N.; Kobayashi, R.; Normand, J.; Raghavachari, K.; Rendell, A.; Burant, J. C.; Iyengar, S. S.; Tomasi, J.; Cossi, M.; Rega, N.; Millam, N. J.; Klene, M.; Knox, J. E.; Cross, J. B.; Bakken, V.; Adamo, C.; Jaramillo, J.; Gomperts, R.; Stratmann, R. E.; Yazyev, O.; Austin, A. J.; Cammi, R.; Pomelli, C.; Ochterski, J. W.; Martin, R. L.; Morokuma, K.; Zakrzewski, V. G.; Voth, G. A.; Salvador, P.; Dannenberg, J. J.; Dapprich, S.; Daniels, A. D.; Farkas, Ö.; Foresman, J. B.; Ortiz, J. V.; Cioslowski, J.; Fox, D. J. *Gaussian 09, Revision A.1*, Gaussian, Inc., Wallingford CT: 2009.